2007 International Symposium on Nonlinear Theory and its Applications
NOLTA'07, Vancouver, Canada, September 16-19, 2007

White Noise Generation with Chaos from Phase-Locked Loop Integrated Circuit Module

Tetsuro Endo and Jun Yokota
Department of Electronics and Communication, Meiji University 1-1-1
Higashi-mita, Tama-ku, Kawasaki-shi, 214-8571, Japan
Email: endoh@isc.maiji.ac.jp

***Abstract*— Recently, the possibility of white noise generation from chaotic PLL has been shown on the basis of numerical simulation. In this paper we demonstrate chaos with the nature of white noise experimentally by using a popular PLL-IC module 4046. This hardware implementation is very easy to handle and many flat power spectra have been obtained at the input of VCO.**

I. Introduction

In this paper, we try to use some type of chaos issued from a phase-locked loop (PLL) as a practical source of white noise in electronic application. At present, noise generators are typically based either on a digitally generated random number sequence or amplified physical noise such as shot noise from the microscopic domain. Chaotic noise derived from a macroscopic system such as a PLL offers advantages as a noise source in that it avoids both the finite repetition interval of digital source and the amplification required of microscopic noise. In [1] it is shown by computer simulation that a sinusoidally-driven PLL can generate chaos of which power spectrum is accurately white over many decades in frequency. Thus a chaotic PLL might serve as a nearly ideal noise generator, with non-repetitive, high-level output and flat power spectrum. The purpose of this paper is to implement such a PLL with practical integrated circuit module 4046. Our experimental results present remarkably flat power spectrum for low frequency region near DC.

II. Heuristic Argument of White Noise Generation Mechanism of PLLs

Chaos from a sinusoidally driven PLL circuit has been extensively investigated by [2]. Hence, we will derive the PLL equation by referring [2]. The PLL can be represented by the block diagram with respect to phase shown in Fig.1. The $\theta_i(t)$ is called the input phase, and the $\theta_o(t)$ is called the output phase. The $\phi(t)$ is called the error phase, and is defined by $\phi(t) = \theta_i(t) - \theta_o(t)$. The nonlinear function $h(\phi)$, a 2π-periodic function of ϕ, is a symmetric triangular characteristics in our case, because our IC module has an EX-OR type phase detector. The $F(s)$ is a low-pass filter (lag-lead filter) with the following transfer function: $F(s) = (1 + \tau_2 s)/(1 + \tau_1 s)$.

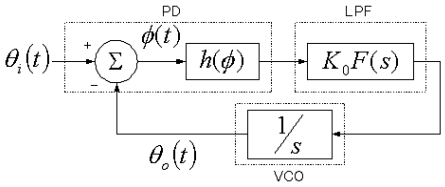

Fig. 1. The phase model of a PLL

From this diagram, one can derive the following differential equation with respect to the error phase.

$$\frac{d^2\phi}{dt^2} + \frac{1}{\tau_1}(1 + K_0\tau_2 h'(\phi))\frac{d\phi}{dt} + \left(\frac{K_0}{\tau_1}\right)h(\phi) = \frac{d^2\theta_i}{dt^2} + \frac{1}{\tau_1}\frac{d\theta_i}{dt} \tag{1}$$

Here we assume that the input signal is modulated by a sinusoidal waveform so that

$$\frac{d\theta_i}{dt} = \Delta\omega + M sin\omega_m t \tag{2}$$

We can define the natural angular frequency (ω_n) and the damping coefficient (ζ) as follows:

$$\omega_n = \sqrt{K_0/\tau_1} \tag{3a}$$

$$\zeta = (1 + K_0\tau_2)/2\sqrt{K_0\tau_1} \tag{3b}$$

We further define the following parameters:

$$\beta = \omega_n/K_0 = 1/\sqrt{K_0\tau_1} \quad \text{normalized natural frequency} \tag{3c}$$

$$\sigma = \Delta\omega/\omega_n \quad \text{normalized frequency detuning} \tag{3d}$$

$$\Omega_m = \omega_m/\omega_n \quad \text{normalized modulation frequency} \tag{3e}$$

$$m = M/\omega_n \quad \text{normalized maximum angular frequency deviation} \tag{3f}$$

By changing the time t into $\tau = \omega_n t$ and replacing τ by t again, (1) and (2) can be normalized to give:

$$\frac{d^2\phi}{dt^2} + \beta\left[1 + \frac{(2\zeta - \beta)h'(\phi)}{\beta}\right]\frac{d\phi}{dt} + h(\phi) = \beta\sigma + \beta m sin\Omega_m t + m\Omega_m cos\Omega_m t \tag{4}$$

where $2\zeta - \beta = K_0\tau_2/\sqrt{K_0\tau_1} \geq 0$. We investigate here the lag filter case in which $2\zeta - \beta = 0$ ($\tau_2 = 0$) for simplicity. By changing the time t into $t = t' - \theta/\Omega_m$ where $tan(\theta) = \Omega_m/\beta$,

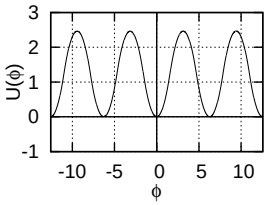

Fig. 2. The potential function $U(\phi)$

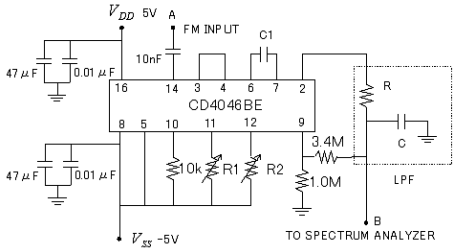

Fig. 3. The practical PLL circuit. The R_1, R_2 and C_1 determine the VCO free-running frequency f_{VCO}.

and replacing t' by t again, equation (4) for the lag filter case becomes the following simpler form.

$$\frac{d^2\phi}{dt^2} + \beta\frac{d\phi}{dt} + h(\phi) = \beta\sigma + asin\Omega_m t \qquad (5)$$
$$a = m\sqrt{\beta^2 + \Omega_m^2}$$

In (5) the 2π-periodic function $h(\phi)$ $(= h(\phi + 2n\pi), n = 0, \pm1, \pm2, ...)$ is given by the following equation

$$h(\phi) = \begin{cases} \phi & \text{for} \quad |\phi| < \frac{\pi}{2} \\ -\phi + \pi & \text{for} \quad \frac{\pi}{2} < \phi < \frac{3}{2}\pi \end{cases} \qquad (6)$$

The dynamics of (5) for small values of "a" is periodic with angular frequency Ω_m; Namely, the phase ϕ is phase-locked with the external signal. However, with the increase of "a", the phase ϕ shows various bifurcations, and at last, it behaves chaotic. Roughly speaking, there are two types of chaos; one is bounded in the ϕ-direction, and the other is unbounded in the ϕ-direction. We will explain the difference by using a particle in a "washboard" potential.

If we define the potential energy U by

$$U(\phi) = \begin{cases} \frac{1}{2}\phi^2 & \text{for} \quad |\phi| < \frac{\pi}{2} \\ -\frac{1}{2}\phi^2 + \pi\phi + \frac{1}{4}\pi^2 & \text{for} \quad \frac{\pi}{2} < \phi < \frac{3}{2}\pi \end{cases} \qquad (7)$$
$$U(\phi + 2n\pi) = U(\phi), n = 0, \pm1, \pm2, ...$$

then (5) with the detuning $\sigma = 0$ for simplicity can be written in the form,

$$\frac{d^2\phi}{dt^2} = -U'(\phi) - \beta\frac{d\phi}{dt} + asin\Omega_m t \qquad (8)$$

which corresponds to Newton's equation for a particle with coordinate ϕ acted on by forces due to the potential $(-dU/d\phi)$, viscous damping $(-\beta d\phi/dt)$, and an external drive $(asin\Omega_m t)$. The washboard potential $U(\phi)$ is illustrated in Fig.2. The origin of white noise in the washboard system can be understood as follow. For a typical chaotic state where ϕ is unbounded, the particle mimics one-dimensional Brownian motion over time scales long compared to the system's characteristic times. Since the particle is strongly influenced by the washboard and sinusoidal drive for times of order $1/\Omega_m$, $1/\omega_0$ ($\omega_0 = 1$: natural angular frequency of the linearized system), and $1/\omega_r$ ($\omega_r = \beta/2$: relaxation angular frequency of the linearized system), it apparently wonders aimlessly to and fro across the washboard over longer times. The diffusive character of this motion results because the particle forgets where it is, the potential being exactly periodic, with every trough identical. The Brownian or diffusive nature of the chaotic motion suggests that, considered over long times, $\phi(t)$ approximates a Wiener-Levy process. Moreover, since the derivative of a Wiener-Levy process yields a white noise process, we expect that the voltage $v = d\phi/dt$ will exhibit a flat power spectrum at frequencies substantially below Ω_m, ω_0, and ω_r [3]. Thus the broadband component of v is expected to be white at low frequencies, and a useful white-noise generator can be realized by using a low-pass filter to remove the unwanted high-frequency components. In contrast, chaos bounded in the ϕ-direction is restricted in one trough of U, therefore, the flow is not diffusive in general and the power spectrum cannot become flat.

III. White Noise Generation Using a Practical PLL

Figuer 3 presents a practical circuit to generate chaos. From Terminal A a carrier signal of which frequency is modulated by a sinusoidal signal ($Msin\omega_m t$ in (2)) is applied. We observe the VCO input voltage at Terminal B. We set that the detuning between the VCO free running frequency and the input carrier frequency is zero for simplicity; namely, $\Delta\omega = 0$. Therefore, τ_1 and τ_2 are given as follows:

$$\tau_1 = CR \quad , \quad \tau_2 = 0 \qquad (9)$$

The D.C. loop gain K_0 satisfies the relation:

$$K_0 = 4f_L \qquad (10)$$

Therefore, by measuring the lock range f_L, one can obtain K_0. In the following experiments, we set each parameter as follows: $f_{VCO} = 46.912$ [KHz], $R = 183.84$ [KΩ], $C = 989.59$ [pF], $\tau_1 = 181926 \times 10^{-9}$ [1/sec], $f_L = 4.371 \times 10^3$ [Hz], $K_0 = 17.484 \times 10^3$ [rad/sec], $\omega_n = 9803.3$ [rad/sec], $f_n = 1560.2$ [Hz], $f_m = 1400$ [Hz], $\omega_m = 8796.4$ [rad/sec] which corresponds to $\sigma = 0$, $\beta = 0.5607$, $\Omega_m = 0.8973$. We observe power spectrum and time waveform of the VCO input voltage, because it is represented as $d\theta_o/dt = Msin\omega_m t - d\phi/dt$. Since $Msin\omega_m t$ is a single spike, we can observe the power spectrum of $-d\phi/dt$ (which is expected to be white for the unbounded chaos) at the input of VCO. Similarly in our computer simulation, we calculate $\dot{\theta}_o = msin\Omega_m t - \dot{\phi}$ in (4) as the VCO input voltage to obtain computer-generated

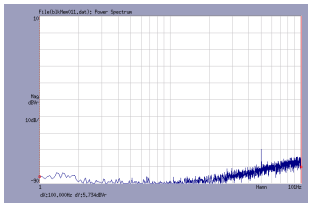

(a)

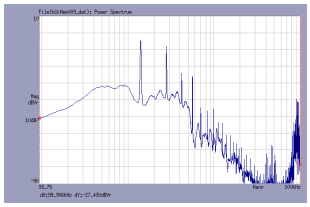

(b)

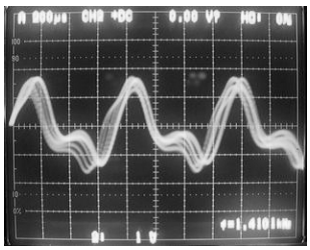

(c)

Fig. 4. The experimentally obtained non-flat power spectrum (a),(b) and the VCO input time waveform (c). (a) abscissa: left margin = 100mHz, right margin = 100Hz; ordinate: lower margin = -90dBV, upper magin = 10dBV. (b) abscissa: left margin = 100Hz, right margin = 100kHz; ordinate: same as (a). (c) The VCO input time waveform. abscissa: left margin = 0s, right margin = 64ms; ordinate: lower margin = -4.472V, upper magin = 4.472V

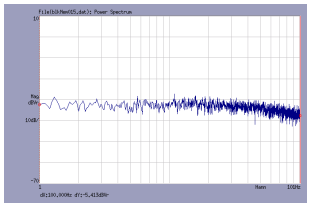

(a)

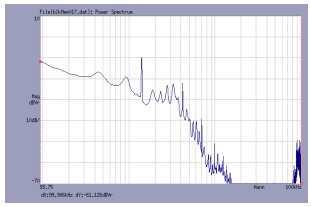

(b)

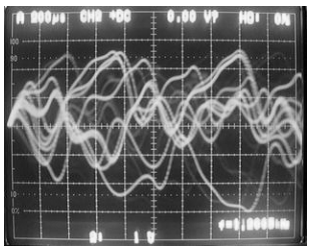

(c)

Fig. 5. The experimentally-obtained flat power spectrum (a),(b) and the VCO input time waveform (c). (a) abscissa: left margin = 100mHz, right margin = 100Hz; ordinate: lower margin = -70dBV, upper magin = 10dBV (b) abscissa: left margin = 100Hz, right margin = 100kHz; ordinate: same as (a). The scales of abscissa and ordinate in (c) are the same as those in Figs.4 (c)

power spectrum. [1] Figs. 4 (a) and (b) show the non-flat power spectrum of chaos observed in our experiments for comparatively small $M = 17404$ [rad/sec] ($m = 1.775$) [2] Figure 4(c) presents the time waveform of the same signal. In contrast, Figures 5(a) and (b) show a power spectrum for chaos observed for $M = 22431$ [rad/sec] $(m = 2.2881)$ which is flat between 0.2 Hz to 100 Hz. Figure 5(c) shows the chaotic time waveform of the same signal. Figures 6(a) and (b) show the computer-generated power spectrum and Lissajous pattern associated with Figs. 4(a) and (b) (only the parameter "m" is slightly modified: $m = 1.740$) Clearly, this chaos is bounded in the ϕ-direction. Figure 7(a) shows the computer-generated spectrum associated with Figs.5(a) and (b). From Fig.7 it is recognized that the spectrum is flat for $\Omega = 6\times10^{-5} \sim 1.5\times10^{-1}$ which corresponds to 0.1 Hz$\sim$230 Hz. Figure 7(b) shows the Lissajous pattern in the $\phi - \dot{\phi}$-plane which clearly shows unbounded chaotic flow in the ϕ-direction.

IV. Practical Design Strategy

From the experiments shown in the previous section, it is confirmed that the power spectrum of the VCO input voltage is almost flat from DC to modulation frequency $f_m(\Omega_m)$.

[1] In practice, there is a gain for PD and VCO. Therefore, the actual VCO input voltage should be $K\dot{\theta}_o$. The factor K is not measured in our experiments. So there is some gain difference between the experiment and the computer simulation.

[2] In Figs. 4(a) and (b) there is about 25 dBV difference in the ordinate. This is due to the bandpass filter characteristics of the spectrum analyzer. The same phenomenon happens for Figs. 5,8 and 9

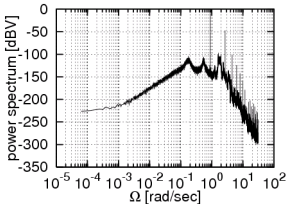

(a)

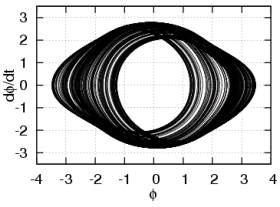

(b)

Fig. 6. The computer-genetated power spectrum (a) and the Lissajous pattern in the ϕ-$\dot{\phi}$ plane (b) associated with Fig.4 Parameters are: $\beta = 0.5607$, $\Omega_m = 0.8973$, $m = 1.740$, $\sigma = 0$ in (4).

Since our purpose is to obtain flat power spectrum for wide frequency range, and since the lower bound of the flat power spectrum seems almost DC, it is desirable to expand the upper frequency limit as large as possible.

For $\sigma = 0$ the shape of power spectrum is determined by parameters β, Ω_m and a in the normalized equation. These parameters correspond to $\omega_n(= \sqrt{K_0/\tau_1})$, ω_m and $A(= M\sqrt{\beta^2 + \Omega_m^2})$ such that: $\omega_n = K_0\beta$, $\omega_m = \omega_n\Omega_m$, $A = \omega_n a$. Therefore, if the power spectrum is flat from D.C. to Ω_m in the normalized equation, it is also flat from D.C. to $f_m(= f_n\Omega_m)$ in the real system. In order to expand the flat power spectrum range, it is necessary to take the natural frequency $f_n = \frac{1}{2\pi}\sqrt{\frac{K_0}{\tau_1}}$ as large as possible for the fixed Ω_m. To do this conjecture, we performed the experiments based on $\sigma = 0$, $\beta = 0.5607$, $\Omega_m = 0.8973$, and $m = 2.2881$ for

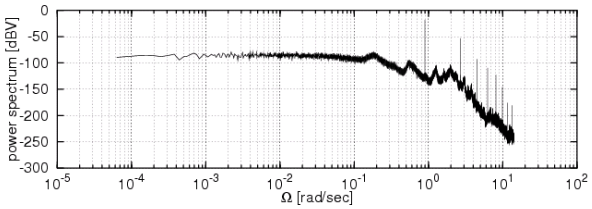

(a)

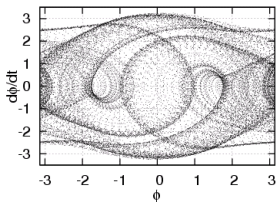

(b)

Fig. 7. The computer-genetated power spectrum (a) and the Lissajous pattern in the ϕ-$\dot{\phi}$ plane (b) assosiated with Fig.9. In (b) ϕ is taken as modulus of 2π. Parameters are: $\beta = 0.5607$, $\Omega_m = 0.8973$, $m = 2.2881$, $\sigma = 0$ in (4).

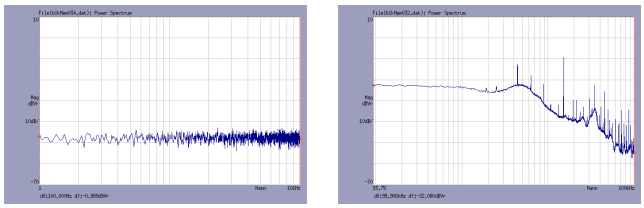

(a) (b)

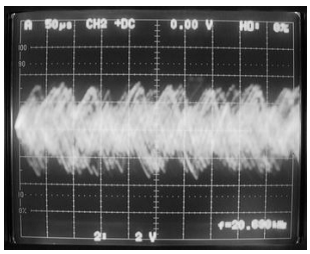

(c)

Fig. 8. The experimentally-obtaind flat power spectrum (a),(b) and the VCO input time waveform (c). The scales of abcissa and ordinate in (a),(b) and (c) are same as those in Figs.5 (a),(b) and (c).

which we obtain reasonable flat power spectrum by computer simulation and experiments (see Figs.5 and 7). According to the above strategy we fix $f_{VCO} = 70.739$ [KHz], $R = 18.089$ [kΩ], $C = 989.59$ [pF], and $f_L = 50.61$ [kHz] which leads to $K_0 = 202.44 \times 10^3$ [rad/sec], $\tau_1 = 17901 \times 10^{-9}$ [1/sec], $\omega_n = 106345$ [rad/sec], $f_n = 16925.3$ [Hz]. Compared to the previous section's experiments, f_n becomes approximately 10.8 times as large as the previous value. In addition we choose $f_m = 15.163$ [kHz] and $M = 243788$ [rad/sec]. From this choice of parameters, the normalized parameters become as: $\sigma = 0$, $\beta = 1/\sqrt{K_0\tau_1} = 0.5253$, $\omega_n = \sqrt{K_0/\tau_1} = 106345.1$ [rad/sec], $m = M/\omega_n = 2.2924$, $\Omega_m = \omega_m/\omega_n = 0.8959$. Figure 8 presents the power spectrum and time waveform for the same β, Ω_m and m. The flat power spectrum expands 20 times as large as that of Fig. 5 (100mHz-2KHz).

At last, we will demonstrate very flat spectrum experimentally obtained for $f_{VCO} = 485.84$ [KHz], $R = 4.703$ [KΩ], $C = 98.643$ [pF], $f_L = 284.47$ [KHz], $f_m = 126.80$ [KHz], $M = 2570.451 \times 10^3$ [rad/sec] ($\beta = 2\zeta = 1.376$, $m = 1.641$, $\Omega_m = 0.5087$ $\sigma = 0$) in Figs.9(a) and (b). It is flat for approximately 0.2 Hz$\sim$100 KHz. [3]

V. Conclusion

We demonstrate chaos with white noise spectrum. Although there is no clear theoretical background, we confirm from our experiments that the unbounded chaos seem more or less to have a flat power spectrum at the VCO input. In our future problem, we will analyze this system more theoretically to establish the design method as a PLL white noise generator.

[3]Unfortunately, since the maximum frequency is 100 [KHz] in our FFT analyzer, we cannot measure the frequency over 100 [KHz], so far.

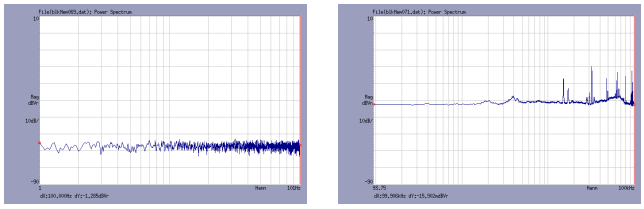

(a) (b)

Fig. 9. The flattest power spectrum obtained in our experiment. The scales of abcissa and ordinate in (a),(b) are same as those in Figs.4 (a),(b).

References

[1] R.L.Kautz, "Using chaos to genetate white noise," Journal of Applied Physics, Vo.86, No.10,pp. 5794-5800 (November 1999).

[2] Tetsuro Endo and Leon Chua, "Chaos from phase-locked loops," IEEE Trans. Circuits and Systems, Vol. 35, No. 8, pp. 987-1003 (August 1988).

[3] M.Inoue and H.Koga, Prog. Theor. Phys. 68, 2184 (1983).